Modeling and design of hybrid Ferromagnetic structures for energy-efficient magnetic sensors

Jofre Herrera Ossó

I. Introduction

Magnetic sensing has been a subject of study since centuries, the main interest through the centuries has been focused in sensing the geomagnetic field for navigation purposes. Nowadays, the interest hasn't declined, neither has the investigation, but the purposes are no longer only centered on navigation but on communication and medical applications among others. For all this purposes it's needed to make it compact, precise and cheaper to manufacture. This new goals lead to several new technologies like Tunnel Magnetoresistance (TMR) [1], Giant Magnetoresistance (GMR) [2], Giant Magnetoimpedance (GMI) [3] and Anisotropic Magnetoresistance (AMR) [4].

The aim of this final degree project is to help design energy-efficient magnetic sensors. The type of magnetic sensors studied are based on anisotropic magnetoresistance. Thanks to this magnetic phenomenon, the AMR sensors will be created only using a thin film of cobalt in which the measurements are taken. In this way, its manufacture and study is simpler than other types of magnetic sensors.

We will focus on systems with a rectangular shape and a thin thickness, where the magnetic field is applied transverse to the length of the material. To understand and study the magnetic structures of these systems, we will perform simulations to evaluate the evolution of magnetic structures inside the sensor. We will work inside the micromagnetism framework, that gives a reliable approximation of the quantum formulation for our dimensions scales.

This final degree project will be divided in two parts. The first part will be exploratory, where the different stable magnetic states of the sensors with different dimensions will be studied. The second part of the study will be a recreation of the experiments conducted at ICMAB regarding AMR sensors. The aim of this part is to study the behavior of the internal magnetic structure of the sensors, that experimentally cannot be directly measured.

II. Study of cobalt magnetic stable states in absence of external magnetic field

In this Section we will study the different stable states depending on the width, the length and the thickness of the material, and also from the initial state, its magnetization. The results will be a phase diagram with the different properties of the stable states found using different configurations. This study will be done executing simulations using the program *Mumax3* [5], each simulation will have different dimensions and initial states, but the material properties will be maintained.

The material properties for the cobalt will be set, following the ones used on [6], at:

$$M_s = 1400\text{kA/m} \quad A_{ex} = 30\text{pJ/m} \quad K_1 = 20\text{kJ/m}^3 \tag{1}$$

The anisotropy vector will be set at z axis, but since the thickness, the z axis, is so thin this anisotropy won't have much effect to the results. The temperature on all the systems will be settled to 0K, so this study will not take into account thermal fluctuations of the magnetization.

The dimensions in study are a width between 62.5nm and 1 μm a length between 62.5nm and 9 μm and a thickness between 3.9nm and 97.66nm. Since *Mumax3* works with cells, the dimension of each cell is set to 500nm/128 which is 3.9nm. Both sets of simulations are computed in only 3 thicknesses, using 1, 13 and 25 cells, then the dimensions of the system regarding width and length are selected to fit the purposes of the investigation. The first set of simulations computed 124 rectangular shapes only covering half of the size range, but the second set of simulations computed 49 different rectangular shapes along all the range of sizes.

The simulations will be done following a simple process: First we set the system dimensions, the width, length and thickness. Then the initial state is imposed to the system. This initial state is not stable, so we leave the state evolving util it reaches a final stable state. The result we get from the final state is the magnetization. In these sets of experiments, the magnetization is presented as a plot of the mean value of the magnetization along the z axis on each point of the plane. Since the magnetization is a vector, the plots have colors regarding the angle in the xy plane and also have some arrows plotted for easy visualization, as can be seen on the initial states of the Figure 1.

The first set of simulations done is starting from an initial state corresponding to a vortex centered on the material, as seen on the Subfigure 1a. Then the system is allowed to relax and find a stable state following the laws of micromagnetism. The second set is done the same way but starting from an initial state saturated parallel to the width of the material, with a little component transverse following the length of the material to break the symmetry, as seen on the Subfigure 1b.

In the plotted results, the mean value of the magnetization in the z axis are relevant since the experimental measurements only measure the mean value of a hole 3d volume, having the mean value across one axis would not be a problem.

A. Simulation set 1: initial vortex magnetization

In this set of simulations, the width is computed from 16 to 240 cells with steps of 32 cells with a total of 8 steps.

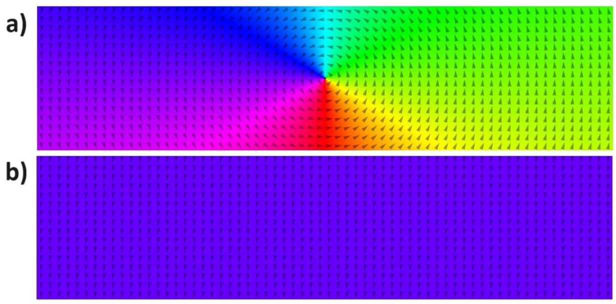

Fig. 1: An example of the initial states of the two sets of simulations, in this case for a cobalt strip of 4μm in length, 1μm in width and 97.66nm of thickness.

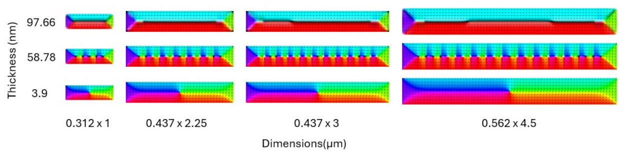

Fig. 2: Different simulations representative of the behavior of the magnetic domains depending on the thickness of the material.

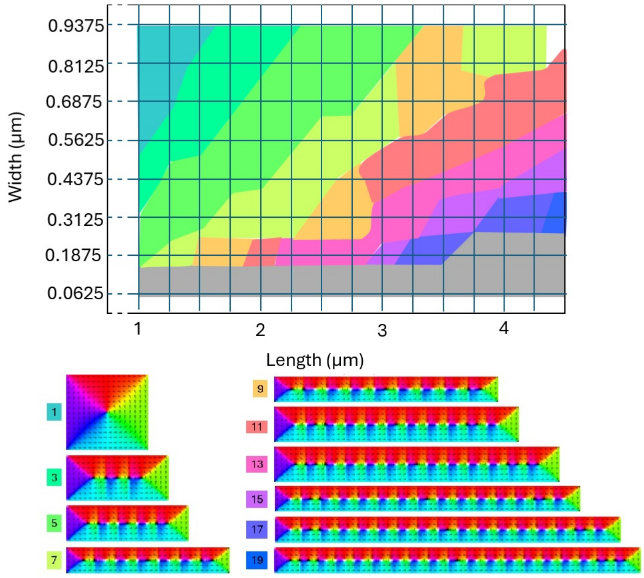

Fig. 3: Phase diagram of the number of stable multidomain structures at a thickness of 50,78nm with an example of each one.

The length is discretized in 15 sections, starting from 256 cells and adding 64 cells for the next simulation.

As seen in the Figure 2, the final stable state, depends strongly on the thickness of the material. With a single layer, a thickness of 3.9nm, all the samples present the same magnetic structure, a centered vortex. With a thickness of 50,78nm the structure creates different number of multidomain regions depending on the relation between the width and length. Finally, with a thickness of 97.66nm the structure creates 4 distinct magnetic domains regardless of the width and length dimensions.

The behavior of this different states strongly dependent on the thickness and do not have a smooth transition between the states. The fact that the states found within the thickness of 50,78nm can only exist within thicknesses ranging between 32.4nm and 89.7nm is highly remarkable since their structure may be interesting for data storage applications.

The total number of multidomain regions stable at thickness 50,78nm is always an odd number and has a clear dependence with the ratio between width and length. In this case, a phase diagram can be done at this thickness regarding the number of stable multidomain structures. In the Figure 3, the different regions correspond to the total number of multidomain structures stable at the states within the regions. It can also be seen a gray region corresponding to states that were not able to show a clear structure of any form due to its small width. In this diagram, an almost linear behavior can be seen regarding the boundary of the different regions as a function of width/length.

B. Simulation set 2: initial uniform magnetization

The width in this set of simulations are measured in cells, and we use five different width each one corresponding to a power of two value, starting from 16 and ending with 256 (corresponding to 1μm). The length is discretized differently, starting with the same powers of two and from 256 making hops of 256 cells, computing only integer numbers of μm in length.

The results of the different simulations, with the highest thickness, 97.66nm, are presented on the Figure 4. Color regions of the diagram are determined manually, since the simulations actually performed are the ones on the vertices of the different discretization values. Each of the three regions correspond to different qualities shared by all stable states inside the region. In the blue region, the stable state is perpendicular to the initial state, and parallel to the easy axis of the system, the width is not great enough to affect the magnetization of the material apart from little perturbations at the vertices. In the green region, the perturbations do not only affect the vertices but the entire width of the ends of the rectangle. This stable state have a vortex on each end, one with a clockwise rotation and the other counterclockwise. The fact that the simulations have the clockwise on the left side and the counterclockwise on the right is due to the angle of the magnetization of our initial state that we introduced to break the symmetry. Finally, on the orange region, the material shows clear magnetic domains. The green and orange regions have a diffuse boundary since, as the Length increases, the magnetic domains stretches until they break leaving the two vortices at the ends. Defining a point where this exact phenomenon is manifested will not make sense, so the boundary is represented blurred. Even taking into account that the boundary is not perfectly defined, certainly we can see the two regions, so using the small data of the simulations an approximate line dividing the regions would have a slope of 0.21, this gives us a ratio to compare with grater systems which cannot fit onto our study.

The same diagram with a thickness of around 50nm the

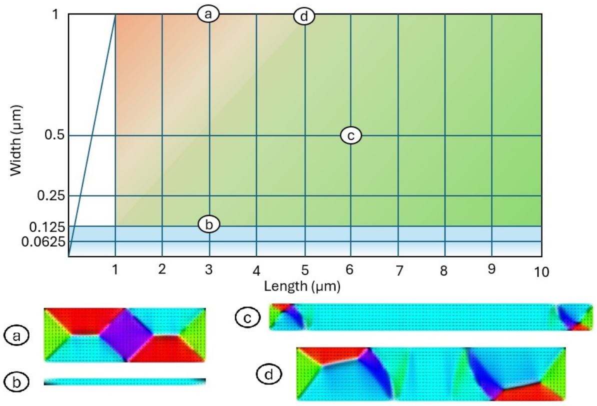

Fig. 4: The phase diagram of the simulations, with a thickness of 97.66nm, from all the simulations. Only 4 simulations are presented showing the main characteristics of each region and one example on the behavior on the simulations on the limit between two boundaries.

three regions still exists but shifted upwards in relation to the higher thickness. The slope of the boundaries does not change remarkably, staying at 0.25. With a thickness of around 4nm, final stable states in all the diagram are uniform states parallel to the length of the material with small perturbations at the ends similar to the blue region. This effect is due to the reduction of the dimensions of the system affecting into the wave function of the particles, allowing them to find less stable states.

III. Study of cobalt magnetic behavior with an applied magnetic field

PHE sensors are being studied at ICMAB by means of magnetoresistance measurements. In this project, simulations will be performed to study the internal magnetic structures formed in the sensors, which cannot be directly measured in experiments. This section describes the experiments conducted at ICMAB by Aleix Barrera and the simulations that I executed to complement the experimental results. The simulations will also be conducted using *Mumax3* using the same material properties as used in the Section II.

A. PHE sensors experiments

The experiments conducted at ICMAB are based on the measurement of the PHE resistance of cobalt bars with a rectangular shape. A current is applied through the length of the material and the PHE resistance is measured perpendicular to it.

Figure 5 (a) shows an optical image of a typical device with a cobalt bar measuring 50 μm in length, 6 μm in width and 100 nm in thickness. Four gold contacts have been grown on top of the Co bar to perform Hall measurements. The devices have been fabricated by optical lithography, sputtering and lift-off.

Using this configuration to make the measurements, the PHE resistance response is obtained at the central part of the cobalt bar. Figure 5 (b) illustrates the variation of the planar Hall resistance of a Co rod as a function of the applied field. The experimental resistance curve exhibits the expected PHE behavior with a linear dependence around zero magnetic field and maximum or minimum values, attributed to an averaged magnetization forming angles of $\theta \pm 45°$ with the current direction.

B. PHE sensors Simulations

The first approximation for simulating the experimental system was to escalate each dimension with a factor 10 since with the original dimensions of 50 μm by 6 μm with a thickness of 100nm the computation time would not be viable. The simulation done was 5 μm by 0.5 μm with a thickness of 11.7nm. The hysteresis simulation is done by changing the norm of the external field in small increments of 0.5mT. This external field is always pointing in the y direction, but with an angle of 1 degree to break the symmetry.

The results of the simulation are presented on the Figure 6. The pink plot is the mean value across the hole sample of the y component of the magnetization m_y for each step of the hysteresis loop. The green plot is the calculated PHE resistance using m_y and m_x.

The results match the experiments conducted at ICMAB, seen at the Figure 5 (b). The magnetization is uniform and its direction (the angle with respect to the Length of the material) change linearly with the change in applied field.

This simulations show the same qualitative dependance as the experimental measurements shown of Figure 5 (b), despite the possible difference between the internal magnetic structure of simulated and experimental bars. To get to this conclusion, we have to take a look at the simulations in the Section II-B that have a strong relation with this one. That simulations found stable states without external magnetic field starting from a saturated state and in these simulations the external magnetic field is reduced slowly, but the state at $B_{ext} = 0$ should be very similar. Reviewing the results of that simulations, we can see that the system of the experiment and the system of the simulation are not in the same region. The simulation is on the blue region where the magnetic state is perfectly parallel to the length, and the experiment, if we extend the diagram, would be on the green region where there are vortex perturbations at both ends of the cobalt bar. From here we can conclude that its behavior will be quite different and does not make sense to escalate the results of the simulation. Even if this simulation cannot correspond to the experiments we meant to reproduce, we can conclude that this setup of the simulation would make a great sensor. However, its creation, due to the small size, would arise technical problems.

1) Simulating systems with higher relation with the experiments.: The next simulation we did, studied a system inside the region where the actual experimental setup was initially. In this simulation, the length and the width are escalated a factor of 10, but the thickness is only escalated a factor of 2. This can be done since seeing the results from the Section II-B, the magnetic states of different systems with very different dimension, inside the same region, were identical.

Since the structures we are working with have vortices at both ends of the thin film, the change of these vortices will not linear nor uniform, so they cannot be used as

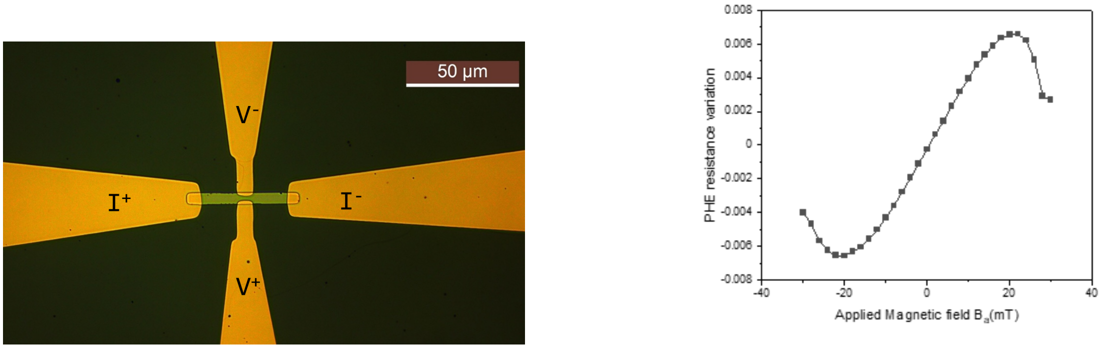

(a) (b)

Fig. 5: a) Optical image of a Cobalt rod with gold electrodes in a PHE configuration. b) Experimental measurements of transversal voltage as a function of the applied magnetic field showing typical PHE behavior, in a Cobalt device with 100nm of thickness, 6um of Width and 50um of length.

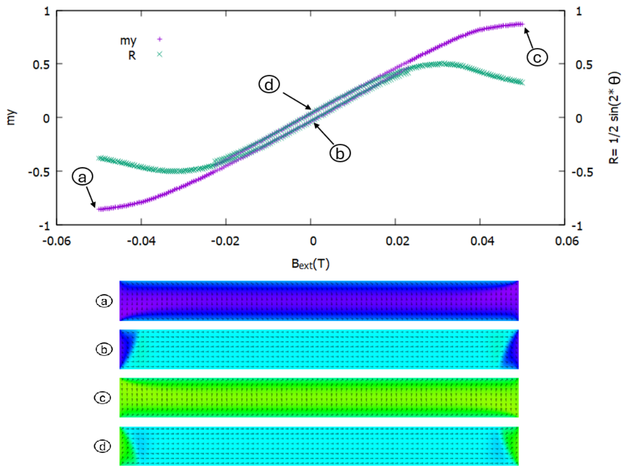

Fig. 6: In this plot are presented the results from a simulation of width 0.5μm, 5μm in length and a thickness of 3.9nm. The data extracted from the simulation is presented on the left y axis, and the normalized PHE resistance calculated from the results is in reference to the right y axis. There are also some intermediate for a better understanding of the hysteresis loop.

sensors. In this new system these behaviors can only be seen at the ends, with the vortices, but if we study the behavior of a thinner region in the middle of the System, the magnetic behaviors should be linear.

The simulation we did with this system started without external field. On each step we increased the external field 0.5mT. In this case we are only interested in the middle part since we are searching a linear behavior, and also the actual experimental measurement were made in the middle part as seen on the Figure 5 (b). Therefore, the results are only calculated using a length of 1 μm at the center of the cobalt strip. The results of these simulations are presented on the Figure 7, where some intermediate states are also presented with the region where the calculations are made is marked.

In these results, we can see that the behavior of the cobalt rod matches perfectly the one measured experimentally until it reaches its maximum at an angle of $45°$, the point where the resistance is no longer plotted. The states *b* and *c* presented show the problem when the angle reaches $45°$, the little perturbations remaining from the

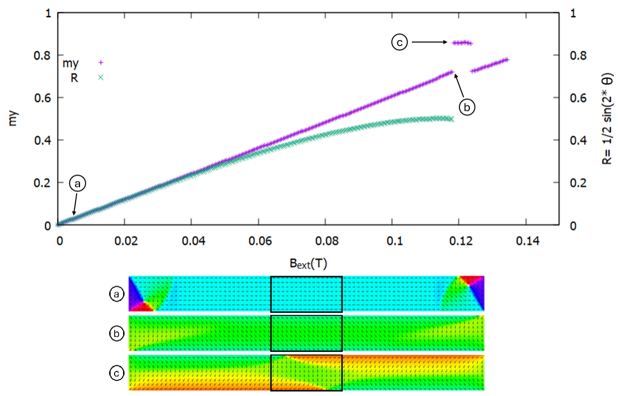

Fig. 7: In this plot are presented the date extracted from the simulation with dimensions: 0.5μm in width, 5μm in length and a thickness of 46.8nm. The left y axis shows the simulation data, and the normalized PHE resistance calculated from the results is in reference to the right y axis. There are also 3 intermediate states presented with the region where the calculations are made is marked

initial vortex collapses into the top and bottom part of the cobalt rod affecting the magnetization along all the length. This phenomenon, regardless of the fact that is not presented on the Section III-A has been observed in several occasions with experimental setups. This fact leads us to conclude that this type of behavior is very dependent on the geometry shape, since on the simulations the rectangles are perfect with sharp corners, but on the experiments the corners cannot be infinitely sharp and cannot be reproduced exactly every time.

IV. Conclusions

The first exploratory part lead us to some interesting conclusions about the behavior of ferromagnetic cobalt strips. On the first set of experiments, starting from a centered vortex, we found a very strong dependence with the thickness of the material. In the other hand, this states that are strongly bonded with the thickness of the material are not easy to modify, making it very protected states which could be useful in information storage.

Starting from a saturated stare, we noted tree very distinct regions where the magnetic stable states shared lots of similarities. In this case, we found that very simple and uniform states are easily created when the dimensions of the material are reduced, but this reduction only needs to take place in one dimensions.

The second part, which is in relation with the experiments conducted at ICMAB granted us a lot of valuable results regarding the behavior of the magnetization of the experiments. The first result to get is independent of the experiments, but we observed that very thin systems cannot form internal structures, which is ideal for PHE sensing applications. Following this same principle, we saw that with systems with higher complexity magnetic structures, PHE sensing cannot be used since the collapse of the structure onto another one will break the linearity.

Finally, studying systems that are on the same region as the experimental one, we managed to get the same results as the experiments. These results lead us to the conclusion that the experimental setup has a uniform magnetization uniform through all the length except in the ends of the cobalt rod, where vortices are formed. With this information, we can see that PHE resistance measurements are independent of the position along the rod, with the exceptions of the ends. With the final simulation, we saw that the ratio between width and length do not affect the results, meaning that any configuration on the green region explained at the Section II-B can be used as a sensor with little to no influence on the results.

References

[1] M. Julliere, "Tunneling between ferromagnetic films," *Physics Letters A*, vol. 54, no. 3, pp. 225–226, 1975. [Online]. Available: https://www.sciencedirect.com/science/article/pii/0375960175901747

[2] G. Binasch, P. Grünberg, F. Saurenbach, and W. Zinn, "Enhanced magnetoresistance in layered magnetic structures with antiferromagnetic interlayer exchange," *Phys. Rev. B*, vol. 39, pp. 4828–4830, Mar 1989. [Online]. Available: https://link.aps.org/doi/10.1103/PhysRevB.39.4828

[3] T. Nakano, M. Oogane, T. Furuichi, and Y. Ando, "Magnetic tunnel junctions using perpendicularly magnetized synthetic antiferromagnetic reference layer for wide-dynamic-range magnetic sensors," *Applied Physics Letters*, vol. 110, no. 1, p. 012401, 01 2017. [Online]. Available: https://doi.org/10.1063/1.4973462

[4] W. Thomson, "Xix. on the electro-dynamic qualities of metals:—effects of magnetization on the electric conductivity of nickel and of iron," *Proceedings of the Royal Society of London*, vol. 8, pp. 546–550, 1857. [Online]. Available: https://royalsocietypublishing.org/doi/abs/10.1098/rspl.1856.0144

[5] A. Vansteenkiste, J. Leliaert, M. Dvornik, M. Helsen, F. Garcia-Sanchez, and B. Van Waeyenberge, "The design and verification of Mumax3," *AIP Advances*, vol. 4, no. 10, p. 107133, 2014. [Online]. Available: http://doi.org/10.1063/1.4899186

[6] V. Kurichenko, D. Karpenkov, and A. Degtyarenko, "Experimental and micromagnetic investigation of texture influence on magnetic properties of anisotropic co/co3o4 exchange-bias composites," *Journal of Magnetism and Magnetic Materials*, vol. 565, p. 170232, 2023. [Online]. Available: https://www.sciencedirect.com/science/article/pii/S0304885322011179